

Modeling and Control of an Electro-Mechanical Ballscrew Actuator for Vibration Active Damping

F. Previdi, *Member, IEEE*, A.L. Cologni, M.G. Madaschi, N. Matteuzzi, M. Nardeschi, S. Toro, S.M. Savaresi, *Member, IEEE*

Abstract — The damping of vibrations on aircrafts and rotorcrafts can provide life extension and weight reduction on those structures on which the vibration load is a significant amount of load endurance spectrum. In this work, a hybrid active-passive inertial actuator system is presented. It is based on a ballscrew based actuator, and the power generation is provided by an open windings three phase motor controlled by a dual inverter. Open windings drives allow to achieve greater torque generation with the same DC bus voltage. The PWM is generated accordingly to a novel algorithm based on a combination of two standard SVM algorithms, one for each inverter. The current controller has been tested on a real test bench at the designed working frequency. Also, a force controller has been designed and tested to verify the force values that can be delivered by the actuator at the designed working frequency.

I. INTRODUCTION

The approaches for vibration reduction are usually divided into two categories: passive damping and active damping methods.

Passive systems use the potential energy generated by the structural response of a material to provide the control force and no energy can be introduced into the system. So, the research on passive vibration damping is mainly focused on materials and mechanical layout to apply effectively the damping force [1-4]. Examples of passive damping materials include viscoelastic materials (VEMs), viscous fluids, magnets, smart materials (piezo-ceramics, electro-rheological fluids, magneto-rheological fluids, magneto-restrictive, shape memory alloys) and high damping alloys. The most commonly used materials are viscoelastic and piezoelectric materials [2,5-6]. Viscoelastic systems dissipate mechanical energy into heat when they undergo cyclic stress due to polymer chain interactions. Piezoelectric actuators are shunted to a passive electric circuit that converts mechanical energy into electricity: so, the passive piezo-circuit system provides an extra-damping to the mechanical system. Passive vibration damping strategies become ineffective when large energy values are required or the dynamics of the system or the frequencies of the disturbance must be changed over time. Moreover, any passive framework can be emulated by an

active control, which may also guarantee finer tuning on the vibration frequency, therefore achieving better performances. This is paid in terms of control design complexity, since only a passive framework is ensured to be stable with respect to any adopted configuration [7,8].

Using active damping it is possible to introduce energy into the system and accurately and effectively achieve the designed performance by means of control systems [7, 9-11]. An active damping system requires sensors, actuators, a source of power and an electronic control system [12]. The use of active damping strategies can provide fine frequency tuning, also varying with time, higher control action intensity, control of power efficiency and greater accuracy in tracking [13]. Moreover, in aerospace applications the actuator must also have small weight and high reliability (see [14] as an example). In particular, active vibration damping systems based on Electro-Mechanical Actuators (EMAs) have been already successfully used, especially in those applications where high force values at quite low frequency are necessary (see [15] as an example).

In this paper, the results about the design and development of a system based on EMA for active vibration damping are presented. The EMA design is of direct drive type, i.e. no gears are interposed between the electric motor and the ballscrew assy. The ballscrew is of the rotating screw-translating nut type. The actuation is provided by a permanent magnet brushless motor, directly connected to the screw shaft. The output force of the actuator is measured by a load-cell on top of the connection rod-end, and linked to a flexible structure (Figs. 1,2). The purpose of the system is to damp the vibrations generated by a vibration of the structure, in order to minimize (nullify) the vibration of the oscillating mass. This concept can be used in a variety of applications, for instance the vibration of the struts connecting an engine to the nacelle or the vibration generated by a propeller on the attachment of the gearbox to the structures [16]. In order to have increased power to mass ratio, strongly advisable in aeronautic applications, the motor has been controlled in open windings [17]. This means that all six of the stator leads are brought out to the external terminals of the machine and they are not Y-connected or Δ -connected. So, the electronic control system needs two inverters and the power flow to the machine can be controlled independently as desired [17]. Multilevel inverters are widely used in high power medium-voltage energy control applications, due to their reduced common mode voltages, high power quality associated with low harmonic distortion. Conventional Space Vector Pulse-Width Modulation (SVPWM) [18-21] has a high computational cost because it ends in a very large number of switching states (64 switches for a standard two level

F. Previdi is with the Dep. of Engineering, Università degli Studi di Bergamo, via Marconi 5, 24044 Dalmine (BG), Italy (phone: +390352052035; e-mail: previdi@unibg.it).

A.L. Cologni, M.G. Madaschi are with the Dep. of Engineering, Università degli Studi di Bergamo.

N. Matteuzzi, M. Nardeschi, S. Toro are with Umbra Cuscineti, Foligno (PG), Italy.

S.M. Savaresi is with the Dept. of Electronics, Computer Engineering and Biomedical Engineering, Politecnico di Milano, Milano, Italy.

inverter). In this work an original and simplified method for SVPWM will be proposed, with a reduced computational cost [22]. A suitable dual inverter electronic control system has been developed and the control algorithm has been implemented and tested in force control loop experiments.

The paper is organized as follows: in Sect. II the mechanical layout of the system is described; in Sect. III the electronic control system SW is presented; in Sect IV the experimental results obtained on a test bench are outlined.



Figure 1. The actuator

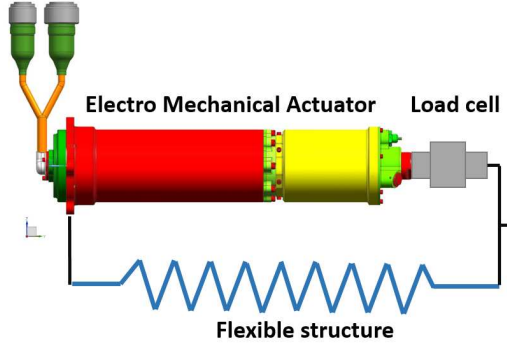


Figure 2. Schematic of the actuator. In red, the electric motor; in yellow the ballscrew; in gray, the load cell; in blue, the passive elastic load.

II. LAYOUT AND MECHANICAL MODEL OF THE ACTUATOR

The actuator has been designed for use in a classic layout for dynamic vibration damping. The damper is connected to an un-damped main mass-spring system, and tuned to the resonant frequency of the main mass-spring. When a force with the same frequency of the tuned resonant frequency of the damping system is applied, there is no motion of the main mass and no net reaction force (other than static equilibrium force) is required at the mechanical constraint. This can be achieved by measuring the vibration force and applying the correct counteracting force with the actuator (Fig. 3).

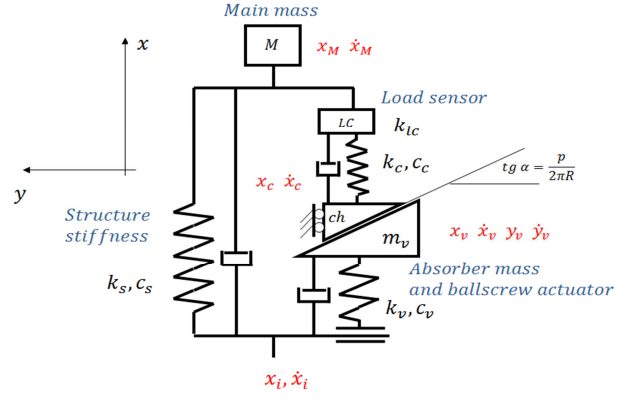


Figure 3. Mechanical model of the system.

The system can be described by the equations of motion of a lumped parameter model. The ballscrew joint can be assumed to be an infinite wedge with angle α (Eqs. 1-3).

$$M \ddot{x}_M = k_s(x_i - x_M) + k_{eq}(x_v + y_v \tan \alpha - x_M) + c_s(\dot{x}_i - \dot{x}_M) + c_c(\dot{x}_v + \dot{y}_v \tan \alpha - \dot{x}_M) \quad (1)$$

$$m_v \ddot{x}_v = k_v(x_i - x_v) - k_{eq}(x_v + y_v \tan \alpha - x_M) + c_v(\dot{x}_i - \dot{x}_v) - c_c(\dot{x}_v + \dot{y}_v \tan \alpha - \dot{x}_M) \quad (2)$$

$$m_{eq} \ddot{y}_v \tan \alpha = -k_{eq}(x_v + y_v \tan \alpha - x_M) - c_c(\dot{x}_v + \dot{y}_v \tan \alpha - \dot{x}_M) \quad (3)$$

where

- M is the main mass;
- m_v is the mass of the actuator;
- k_s and c_s are respectively the elastic constant and the damping coefficient of the load spring;
- k_c and c_c are respectively the elastic constant and the damping coefficient of the load sensor;
- k_v and c_v are respectively the elastic constant and the damping coefficient of the connection between the sensor and the actuator;
- k_{LC} is the elastic constant of the load sensor;
- $k_{eq} = \frac{k_c \cdot k_{LC}}{k_c + k_{LC}}$ is the equivalent elasticity of the load sensor and its connection to the actuator.

The equivalence of the rotating motion to the translating motion is given by the following equivalence that put in relation the moment of inertia of the rotating mass to a linear inertia

$$m_{eq} = \frac{4\pi^2 J}{p^2} \quad (4)$$

being J the rotating mass inertia and p is the screw pitch.

The study of the system response validates the principle of vibration damping in the neighborhood of a resonant frequency that can be tuned by a proper design choice of the ballscrew pitch and actuator stiffness. In particular, a natural frequency has been observed, corresponding to the natural frequency of the actuator mass and overall stiffness.

The EMA main requirement is to provide a sinusoidal force with a variable amplitude between 0 and an assigned value F_{max} , at a specific working frequency f_w . The external

load is basically of elastic nature and represented by the stiffness of the flexible structure where the actuator is assembled (Fig. 4).

The designed actuator is very light and compact (external diameter 80 mm; length 350 mm; weight 6.5 kg) and connected to a DC BUS at 28 V can provide up to 750 W with a very high efficiency (greater than 80%), achieved thanks to the dual inverter architecture.

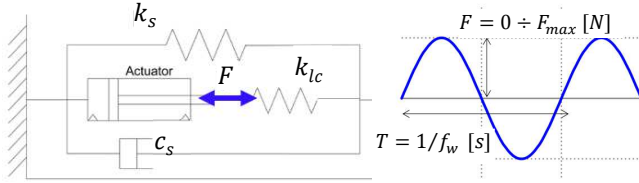


Figure 4. Schematic representation of the desired operating conditions of the actuator.

III. SPACE VECTOR PULSE-WIDTH MODULATION (SVPM) OF A DUAL INVERTER ELECTROMECHANICAL ACTUATOR

The control system is based on two nested control loops. The inner one is the current control systems. The second one is a force controller (see Sect. IV). In this paper, an original current control algorithm for multilevel inverters is presented. In order to drive the system, a multilevel electronic inverter has been designed. Multilevel inverters can have increased output voltage amplitude with respect to standard inverters and they can reduce the current harmonic content and the switching frequency to which the switches are subjected. The two most popular techniques for the generation of PWM in multilevel inverters are sine-triangle PWM (SPWM) and Space Vector PWM (SVPWM) [18-21]. SPWM involves the comparison of a reference signal with a number of level shifted carriers to generate the PWM signal. SVPWM involves synthesizing the reference voltage space vector by switching among the three nearest voltage space vectors. The PWM techniques complexity and computational cost increase with the number of levels of the inverter.

The schematic diagram of an open-end winding dual inverter for brushless motor is shown in Fig 5. Top and bottom switches are working in a complementary mode. So, the switching vector for three phases must take into account that when the value 1 is assigned to the "ON" state of the top switch, the value 0 is assigned to the "ON" state of the bottom switch. The combination of the switch configurations for the two inverters yields 64 possible switches states for the whole dual-level inverter, corresponding to 18 different output voltage vectors and a null vector and 24 sectors, as represented in Fig. 6. By using the SVM technique, these voltage vectors can be combined to obtain any output voltage vector lying inside the outer hexagon, by defining suitable duty cycle ratios and a procedure to correctly identifying the sector number (Fig. 7).

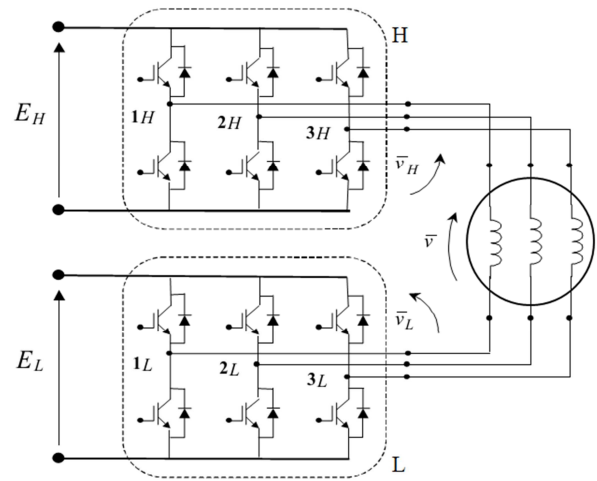


Figure 5. Schematic representation of a dual inverter.

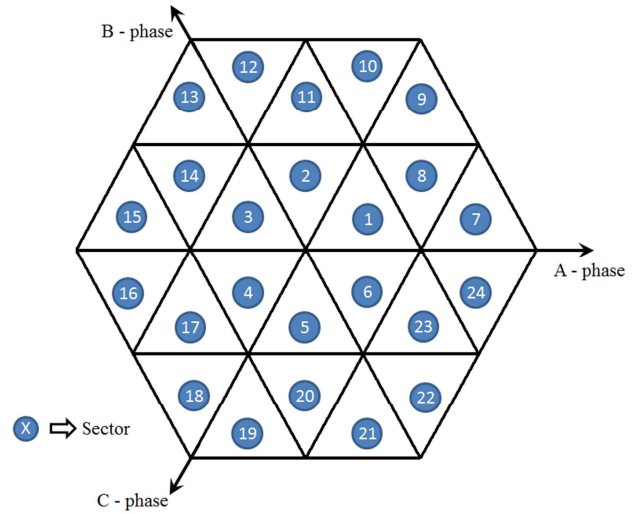


Figure 6. Resultant sector representation of the SVPWM for a dual inverter.

To achieve this purpose it's necessary to study in depth the space of vectors in Figs. 6-7. It is possible to notice that the hexagon of the resultant space vectors combination can be created using only some combinations and not all of them. So, it is possible to simplify the number of combinations and use them efficiently. For instance, the vectors in sectors 1,7,8,9 in Fig. 6 can be obtained by four combinations $\{1,4\}$, $\{2,4\}$, $\{1,5\}$, $\{2,5\}$ in Fig. 7, so identifying a unique macro-sector (in blue in Fig.8), where for the inverter H the active space vectors are 1 and 2, and for the inverter L the active space vectors are 4 and 5, which are the opposite vectors with respect to those of inverter H.

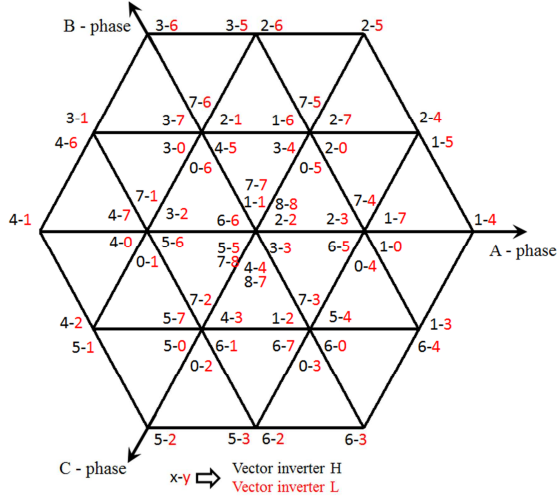


Figure 7. Resultant space vector combination.

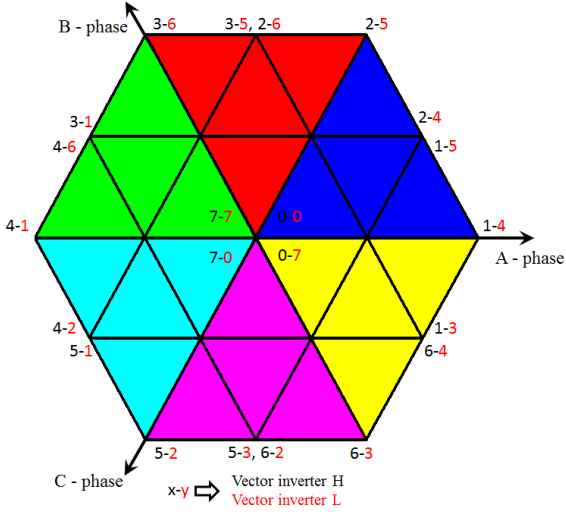


Figure 8. Simplified algorithm for the selection of the desired sector.

Therefore, in order to apply these couples of space vectors, it is necessary to be sure that inverter *L* computes always the opposite space vectors of inverter *H*. To do this, it is enough to use standard SVM, but feeding it with negated signals. In this way the generation of PWMs is very simple, since it is possible to reuse the standard SVM, provided that some constraints are fulfilled. Finally, to control efficiently the current, it is necessary to use the complete Clarke and Park transform, because the system can be not balanced.

In Fig. 9, the current loop control scheme for the motors with open-end windings is shown [22]. Direct and quadrature currents are computed by means of a suitable matrix transformation and they are regulated by means of PI controllers. The generated control action is transformed into voltages in the α, β frame which are transformed into PWM signal by the SVM algorithm described before.

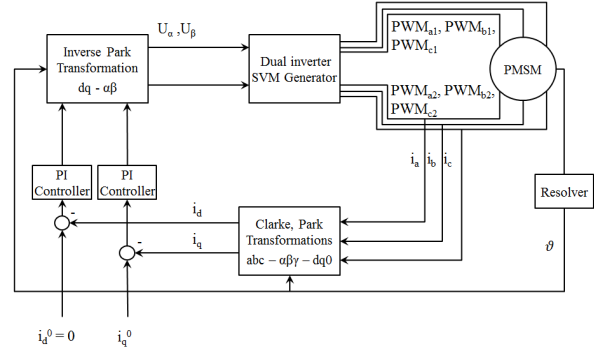


Figure 9. Schematic representation of the current control system.

IV. EXPERIMENTAL RESULTS

The actuator has been tested on a test bench with an elastic load. The actuator performance has been assessed in experiments at the target working frequency f_w , by measuring the generated force, the kinematic parameters (angular and linear displacement/velocity/acceleration) and current/power absorption.

In this section, results are shown in terms of normalized variables for confidentiality reasons. More specifically, the applied force is normalized to the maximum force amplitude. The currents are defined as submultiples of the current sensors full-scale. The frequency is normalized to the design working frequency f_w . The time scale is defined in terms of multiples of $1/f_w$.

The tracking performance is evaluated by means of the Relative Mean Squared Error, i.e.

$$RMSE = \frac{\sum_{t=1}^N e^2(t)}{\sum_{t=1}^N y^2(t)} \quad (4)$$

Where: $y(t)$ is the tracking measure, $e(t)$ is the tracking error and N is the number of samples. The RMSE can assume values greater than 0, being 0 when the tracking is perfect.

The current and force control loops have been tested separately using sinusoidal reference signal at the frequency f_w . First of all, the current control loop has been tested using as a reference a sinusoidal quadrature current and a null direct current. In fact, the quadrature current is directly related to the generated torque, while the direct current represent the power losses. The results in terms of current tracking are shown in Figs. 10,11. Notice that the quadrature current is perfectly in phase with the reference and the quality of the tracking is very high. The RMSE of the considered experiment is 0.0236. The direct current is slightly oscillating close to zero, because of a not perfect compensation of back electromotive force out of the control loop bandwidth. The RMSE of the considered experiment is 0.0113.

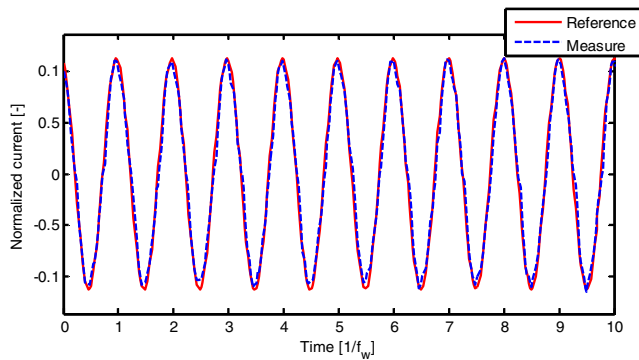


Figure 10. Sinusoidal tracking of the quadrature current.

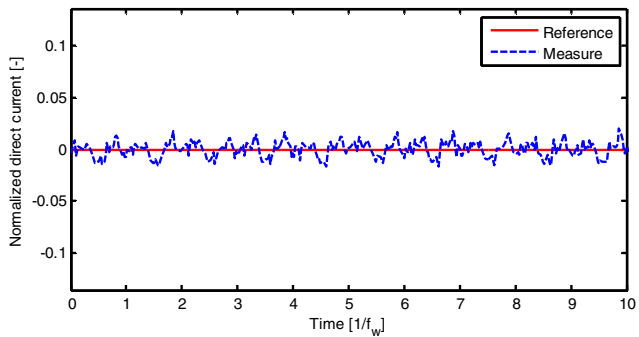


Figure 11. Residual direct current due to bmf effects.

As expected the rotor position is perfectly has a behavior very similar to the quadrature current. In Fig. 12, the normalized angle at the motor shaft is shown, as measured by the motor resolver.

The depicted behavior has a very strong meaning: it denotes the linearity of the system in the test conditions; for this reason, it is possible to close an external control loop with a linear regulator.

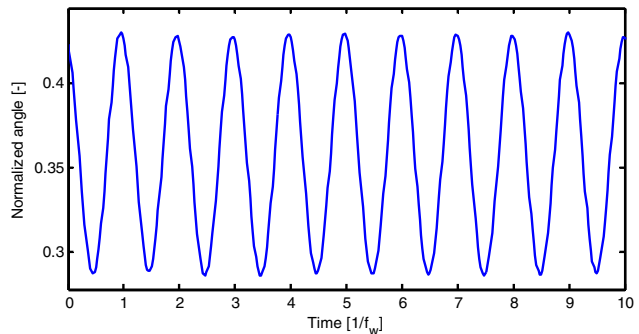


Figure 12. Motor resolver measurement during the current control loop test.

In order to test the effective efficiency of the overall system a PI force controller has been designed, tuned and implemented. First of all, the static and dynamic response of the system with input the reference quadrature current (the current control loop is active) and output the measured force has been evaluated. In Fig. 13, the relationship between the peak force and reference quadrature current is shown during experiments with sinusoidal input at the designed working frequency f_w . As expected, there is a linear relationship

between the actuated force and the reference current of the current control loop. In Fig 14, the dynamic response has been estimated by means of a frequency sweep input with a frequency range up to 1.5 times the design working frequency. The experiment has been performed using a normalized current amplitude of 0.085.

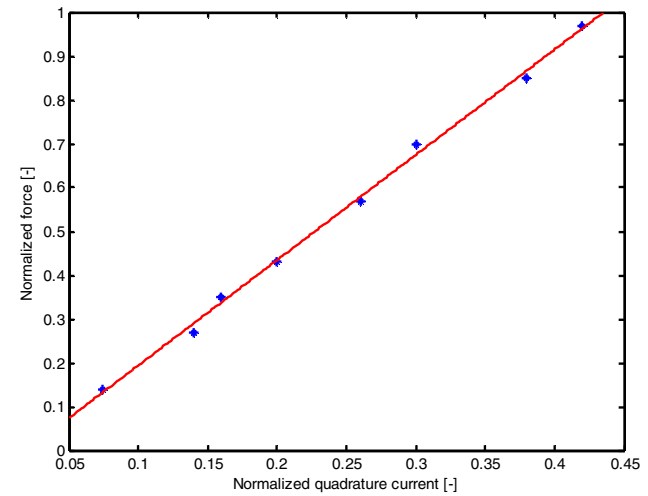


Figure 13. Relationship between the maximum amplitude of the actuated force and the maximum amplitude of the applied reference quadrature current measured with a sinusoidal input at the design working frequency.

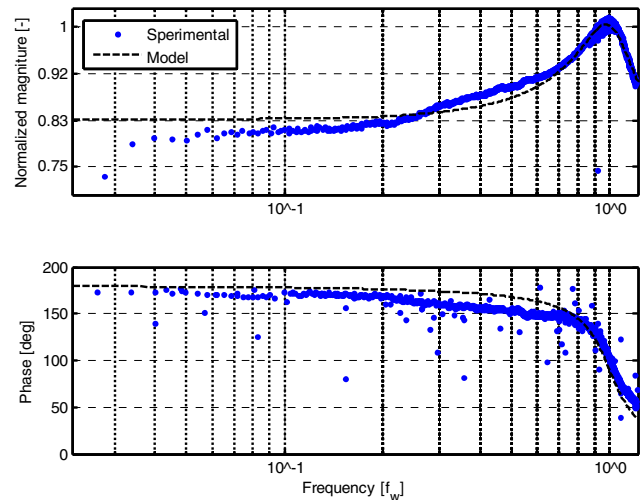


Figure 14. Estimated frequency response diagrams between reference quadrature current (input) and actuated force (output).

As it can be noticed, the real behavior of the system is very similar to the theoretical; it is important to underline that, in terms of phase, there is a negative gain between the current and the applied force.

Finally, a closed loop force tracking experiment has been performed with a sinusoidal reference signal at the design working frequency (Fig 15). The force tracking is very good; in fact the force RMSE is 0.0780. As it can be observed, the negative side of the force has, partially, a different shape in respect to the positive one. This behavior will be investigated in the future.

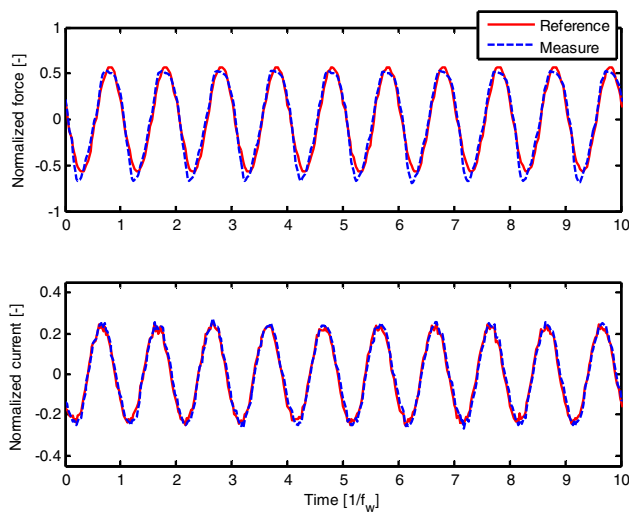


Figure 15. Force closed loop tracking with sinusoidal reference at the design working frequency.

Finally, it is worth noting that the energy flow between the actuator and the structure goes in both directions: when the actuator is compressing the load spring, the energy flows from the motor to the structure; when the spring extends, the elastic energy stored in the spring is released to the actuator in a regenerating phase and energy could be stored in an accumulator.

V. CONCLUSIONS

In this work, an electromechanical actuator using a ballscrew to transmit motion has been designed and effectively used in an experimental test bench for vibration damping.

The actuator is driven by a three phase motor with open windings, using a dual-inverter to control the phase currents. The SVPWM current control is based on a novel simplified algorithm that provides very good actuation properties with small computation burden. Using this solution 70% more power is available with the same voltage supply with respect to a traditional Y-connected motor.

A proper mechanical design of the ballscrew and the actuator stiffness provides a strong linearity between the delivered current and the actuated force, also in open loop. The force control loop finally provides very good tracking performances of the force profiles at the design working frequency. Linearity of the actuator has been validated on a high range of frequencies and forces.

Further investigations will be dedicated to the regenerative aspects of elastic energy stored in the structure during motoring phase of the actuator and released by the structure to the actuator during the aiding phase.

REFERENCES

[1] J. Q. Sun, Jolly M. R., Norris, M. A., "Passive, Adaptive and Active Tuned Vibration Absorbers—A Survey", *Journal of Mechanical Design*, vol. 117(B), pp. 234-242, 1995.
 [2] S.Y. Wu, "Multiple PZT Transducer Implemented with multiple-mode piezoelectric shunt for passive vibrating damping", *Proc. of the SPIE*

Symposium on Smart Structures Materiales Passive Damping Isolation, pp. 113-122, 1999.

[3] N.W. Hagood and E.F. Crawley, "Experimental Investigation of Passive Enhancement of Damping for Smart Structure", *AIAA Journal of Guidance, Navigation and Control*, vol. 1, no. 3, pp. 327-354, 1991.
 [4] J. P. Den Hartog, *Mechanical vibrations*, Courier Dover Publications, 2013.
 [5] S.O.R. Moheimani, "A survey of recent innovations in vibration damping and control using shunted piezoelectric transducers", *IEEE Trans. on Control Systems Technology*, vol. 11, no. 4, pp. 482-494, 2003.
 [6] M.D. Rao, "Recent applications of viscoelastic damping for noise control in automobiles and commercial airplanes", *Journal of Sound and Vibration*, vol. 262, no. 3, pp. 457-474, 2003
 [7] M.J. Balas, "Feedback Control of Flexible Systems", *IEEE Transaction on Automatic Control*, vol. AC-23, no. 4, pp. 673-679, 1979.
 [8] C.R. Fuller, S.J Elliot and P.A Nelson, *Active Control of Vibrations*, Academic Press Limited, London (UK), 1996.
 [9] J. Dosch, D.J. Inman and E. Garcia, "A Self-Sensing Piezoelectric Actuator for Collocated Control", *Journal of Intelligent Materials Structures*, vol. 3, no. 1, pp. 166-185, 1992.
 [10] E.H. Anderson, N. Hagood and J.M. Goodliffe, "Self Sensing Piezoelectric Actuators. Analysis and Application to controlled structures", *Proc. of Structures, Structural Dynamics, Materials Conference*, Dallas (TX), pp. 2141-2155, 1992.
 [11] P. Vallone, "High Performance Piezo-Based Self Sensor for Structural Vibration Control", *Proc of SPIE Conference on Smart Structures Integrated Systems*, pp. 643-655, 1995.
 [12] N. Vahdati, Pike J.A. (1993), "Analytical Comparison of Active Versus Passive Aircraft Engine Suspensions", *Proc. of 2nd Conference on Recent Advances in Active Control of Sound and Vibration*, Blacksburg, VA (USA), 1993.
 [13] F. Previdi, C. Spelta, M.G. Madaschi, D. Belloli, S.M. Savaresi, F. Fagnoli, E. Silani, "Active vibration control over the flexible structure of a kitchen hood", *Mechatronics*, accepted for publication, DOI: 10.1016/j.mechatronics.2014.01.010, 2014.
 [14] A. Garcia, J. Cusido, J. Rosero, J. Ortega and L. Romeral, "Reliable Electro-Mechanical Actuators in Aircraft," *Aerospace and Electronic Systems Magazine*, vol. 23, no. 8, pp. 19 - 25, Aug. 2008.
 [15] K. Nakano, Y. Suda, S. Nakadai, "Self-powered active vibration control using a single electric actuator", *Journal of Sound and Vibration*, vol. 260, no. 2, pp. 213-235, 2003.
 [16] J.P. Henderson, Plummer A., Johnston N., "Hybrid Active-Passive Electro-Hydrostatic Vibration Isolation for Rotorcraft", *Proc. of Recent Advances in Aerospace Actuation Systems and Components*, Toulouse (FRA), pp. 44-50, 2012.
 [17] M-S Kwak and S-K Sul, "Flux weakening control of an open winding machine with isolated dual inverters", *Proc of the 42nd IAS Annual Meeting, Industrial Applications Conference*, pp. 251-255, 2007.
 [18] N. Celanovic, Boroyevich D., Skudelny H. C. and Stanke G. V., "A fast Space Vector Modulation algorithm for multilevel three-phase converters", *IEEE Transaction on Industry Application*, vol.37, no. 2, pp. 637 - 641, 2011.
 [19] A.K. Gupta and Khambadkone A., "A Space Vector PWM Scheme for Multilevel Inverters Based on Two-Level Space Vector PWM", *IEEE Transaction on Industrial Electronics*, vol.53, no. 5, pp. 1631-1639, 2006.
 [20] H.W. Van Den Broeck, Skudelny H. C. and Stanke G. V. (1988), "Analysis and Realization of a Pulsewidth Modulator Based on Voltage Space Vectors", *IEEE Transaction on Industry Application*, vol. 24, no. 1, pp. 142-150, 1988.
 [21] Y. Kawataba, M. Nasu, T. Nomoto, E.C. Ejiogu, T. Kawabata, "High-efficiency and low acoustic noise drive system using open-winding AC motor and two Space Vector Modulated inverters", *IEEE Trans. on Industrial Electronics*, vol. 49, no. 4, pp.783-789, 2002.
 [22] M.G. Madaschi, Gryazina E., Cologni A. L., Spelta C., Previdi F., Savaresi S. M. and Pesenti I., "Robust control of magnetic guidance lightweight AGVs path tracking using randomization methods", *Proc. of European Control Conference*, Zurich (SUI), pp. 262-267, 2013.